

## Temporal Dynamics of Tyrosine Phosphorylation in Insulin Signaling

Running title: Tyrosine phosphorylation in insulin signaling

Katrin Schmelzle<sup>#</sup>, Susan Kane<sup>§</sup>, Scott Gridley<sup>§</sup>, Gustav E. Lienhard<sup>§</sup>, and Forest M. White<sup>#\*</sup>

<sup>#</sup>Biological Engineering Division, MIT, Cambridge MA 02139; <sup>§</sup>Biochemistry Department, Dartmouth Medical School, Hanover NH 03755

\* Corresponding author:

Forest M. White  
77 Massachusetts Ave  
56-787a  
MIT  
Cambridge, MA 02139

Phone: 617-258-8949  
Fax: 617-258-0225  
e-mail: fwhite@mit.edu

Abbreviations: APS, adaptor protein with pleckstrin homology and src homology 2 domains; EGF, epidermal growth factor; ERK, Extracellular signal-regulated kinase; Gab, GRB2-associated binding protein; IMAC, immobilized metal affinity chromatography; IRS, insulin receptor substrate; LC-MS/MS: liquid chromatography tandem mass spectrometry; MAPK, mitogen-activated protein kinase; PI3K, phosphatidylinositol 3-kinase; PTRF, polymerase I and transcript release factor; pTyr, phosphorylated tyrosine; SHC: Src homology 2 domain containing transforming protein C; SHP-2, protein tyrosine phosphatase, non-receptor type II

This is an author-created, uncopyedited electronic version of an article accepted for publication in *Diabetes* (<http://diabetes.diabetesjournals.org>). The American Diabetes Association (ADA), publisher of *Diabetes*, is not responsible for any errors or omissions in this version of the manuscript or any version derived from it by third parties. The definitive publisher-authenticated version is available online at [\[URL\]](#).

## **Abstract**

The insulin signaling network regulates blood glucose levels, controls metabolism, and when dysregulated, may lead to the development of type 2 diabetes. Although the role of tyrosine phosphorylation in this network is clear, only a limited number of insulin-induced tyrosine phosphorylation sites have been identified. To address this issue and establish temporal response, we have, for the first time, carried out an extensive, quantitative, mass spectrometry-based analysis of tyrosine phosphorylation in response to insulin. The study was performed with 3T3-L1 adipocytes stimulated with insulin for 0, 5, 15, and 45 min. It has resulted in the identification and relative temporal quantification of 122 tyrosine phosphorylation sites on 89 proteins. Insulin treatment caused a change of at least 1.3-fold in tyrosine phosphorylation on 89 of these sites. Among the responsive sites 20 were previously known to be tyrosine phosphorylated with insulin treatment, including sites on the insulin receptor and IRS-1. The remaining 69 responsive sites have not previously been shown to be altered by insulin treatment. They were on proteins with a wide variety of functions, including components of the trafficking machinery for the insulin-responsive glucose transporter GLUT4. These results show that insulin-elicited tyrosine phosphorylation is extensive, and implicate a number of hitherto unrecognized proteins in insulin action.

## Introduction

Metabolic control is primarily regulated by the insulin signaling network. In healthy individuals, insulin stimulates glucose uptake from the bloodstream into adipose tissue and skeletal muscle while inhibiting glucose production in the liver. Dysregulation of this network associated with insulin resistance causes an increase in blood glucose and lipid levels, often initially associated with an increase in insulin levels and eventually culminating in type 2 diabetes (1). Understanding the signaling network activated by insulin stimulation is crucial for identifying the causes and effects of network dysregulation and insulin resistance.

Insulin binds to the insulin receptor at the cell surface and activates its tyrosine kinase activity, leading to autophosphorylation and phosphorylation of several receptor substrates. Phosphorylation of selected tyrosine sites on receptor substrates are known to activate different pathways leading to increased glucose uptake, lipogenesis, and glycogen and protein synthesis , as well as to stimulation of cell growth (1; 2). In addition to activation of these pathways by tyrosine phosphorylation, several mechanisms of downregulating the response to insulin stimulation have also been identified. For instance, serine phosphorylation on IRS-1 induced by a variety of factors has been shown to interfere with the activating effects of tyrosine phosphorylation, by decreasing binding to the insulin receptor or increasing degradation of IRS-1(1; 3; 4). Ser/Thr phosphorylation of the insulin receptor has also been shown to decrease tyrosine kinase activity (1). Downregulation of the insulin receptor (1) and IRS-1 (3) are two additional mechanisms of mediating insulin resistance. Many of these factors are reflected in decreased amounts of the tyrosine phosphorylated receptor and receptor substrates

with concomitant reduction in downstream signaling. Even though tyrosine phosphorylation plays a key role in insulin signaling, rather limited knowledge of specific phosphorylation sites, mainly focusing on tyrosine phosphorylation on the insulin receptor and IRS-1, is available so far. Therefore, we expected that a more comprehensive analysis of tyrosine phosphorylation upon insulin stimulation would lead to further insights into the biology of the signaling network.

We have recently developed a mass spectrometric methodology for the identification and quantification of tyrosine phosphorylation sites on many proteins (5). Here we have applied this methodology to the analysis of insulin signaling in 3T3-L1 adipocytes stimulated with insulin for 0, 5, 15, or 45 minutes. Using this approach, we were able to identify and quantify the temporal dynamics of many previously described sites on the insulin receptor and several insulin receptor substrates, as well as many additional sites, both previously characterized and novel, on other proteins associated with insulin signaling. These include sites related to the mitogen-activated protein kinase (MAPK) and phosphatidylinositol 3-kinase (PI3K) pathways. Moreover, this analysis also produced temporal phosphorylation profiles for a number of novel phosphorylation sites on proteins which have, so far, not been directly associated with insulin signaling, such as proteins in the machinery of GLUT4 trafficking. The results of this study show that the insulin-elicited increase in tyrosine phosphorylation is more widespread than previously known, and identify many new sites to be explored for their specific roles in insulin action.

## **Materials and Methods**

### **Cell culture, insulin stimulation and cell lysis**

3T3-L1 fibroblasts from the American Type Culture Collection were carried as fibroblasts and differentiated into adipocytes, as described previously (6). Confluent 10-cm plates of adipocytes at day 7 after differentiation ( $\sim 1 \times 10^7$  cells per 10 cm plate) were washed with serum-free DMEM and incubated in serum-free DMEM with 1 mg/ml bovine serum albumin for 16 hours. Cells were then stimulated with 150 nM insulin in this medium for 5 min, 15 min and 45 min; non-treated cells were used as 0 min time point. For every time point, 3 plates were prepared. After rinsing with PBS, cells were lysed in 1.5 ml 8 M urea containing 1 mM  $\text{Na}_3\text{VO}_4$  (7) ; the cell lysate was frozen in liquid nitrogen and stored at  $-70^\circ\text{C}$  until further use.

### **Sample processing and peptide immunoprecipitation**

Protein concentration was determined by BCA assay (Pierce). Proteins were reduced, alkylated and digested with modified trypsin (Promega, enzyme:substrate ratio 1:50) (5). The digest was acidified to pH 2 with HCl, centrifuged, and the supernatant was filtered (Millex-HV filter, 0.45  $\mu\text{m}$  pore size, Millipore), desalted and fractionated on a C18 Sep-Pak Plus Cartridge (Waters). Peptides eluted with 25% acetonitrile in 0.1% acetic acid were lyophilized, labeled with iTRAQ (1/4 plate per condition), combined, and phosphotyrosine (pTyr) peptide immunoprecipitation was performed with anti-pTyr antibodies as previously described (5), in 30 mM TrisCl, 30 mM NaCl pH 7.4 containing 0.4% Nonidet P40 Substitute (Fluka). For peptide immunoprecipitation, a mixture of P-Tyr-100 (Cell Signaling #9411, 18  $\mu\text{g}$ ) and PT-66 (Sigma P3300, 12  $\mu\text{g}$ ), previously coupled to Protein G Plus-Agarose beads (Calbiochem, 20  $\mu\text{l}$ ) was used, with the

peptides derived from one 10-cm plate in 0.45 ml. Bound peptides were eluted from the antibody with 70  $\mu$ l glycine 100 mM, pH 2.1.

### **Chromatography and LC-MS/MS**

Since peptide immunoprecipitation with pan-specific anti-phosphotyrosine antibodies is subject to non-specific binding (specifically, those peptides containing aromatic amino acids (e.g. tyrosine, phenylalanine, tryptophan) appear to be preferentially enriched), further enrichment for phosphopeptides was performed using immobilized metal affinity chromatography (IMAC), as previously described (5). This tandem affinity strategy virtually eliminated non-specifically retained peptides, such that almost all peptides in the final analysis contained phosphorylated tyrosine. Phosphopeptides were eluted from the IMAC column to a capillary precolumn (100  $\mu$ m I.D., packed with 10  $\mu$ m ODS-A (Kanematsu)), which was then connected to a capillary analytical column (50  $\mu$ m I.D. packed with 10 cm of 5  $\mu$ m ODS-AQ (YMC-Waters)) with an integrated, laser-pulled (Model P-2000, Sutter Instrument Co) electrospray ionization emitter tip (about 2  $\mu$ m diameter) (8). Peptides were eluted (flow rate ~20 nl/min) from the liquid chromatography (LC) column to the quadrupole time-of-flight mass spectrometer (QSTAR XL, Applied Biosystems) with the following gradient: 0 min: 0% B, 10 min: 13% B, 105 min: 42% B, 115 min: 60% B, 122 min: 100% B (solvent A = 0.2 M acetic acid and solvent B = 70% acetonitrile, 0.2 M acetic acid). Data was acquired in information-dependent acquisition mode, in which a full scan mass spectrum (2.5 s) was followed by tandem mass spectrometry (MS/MS) of the 4 most abundant ions (4 s each) of charge state 2-5 using mass exclusion time of 25 s.

### **Phosphopeptide Sequencing and Quantitative Analysis**

MS/MS spectra were extracted and searched against rodent (mouse and rat) protein database (NCBI) using ProQuant (Applied Biosystems) as described previously (5). Mass tolerance was set to 2.2 atomic mass units for precursor ions and 0.15 atomic mass units for fragment ions. Phosphotyrosine-containing peptides were manually validated and quantified. Peak areas for each of the four signature peaks ( $m/z$ : 114, 115, 116, 117) were obtained and corrected according to the manufacturer's instructions to account for isotopic overlap. Only spectra with signature peaks below 1500 counts were considered for quantification. To compensate for small differences in the sample amounts at each time point, the results were normalized to those for non-phosphorylated peptides of 10 abundant proteins present in the samples (supplementary material, Table 1). Finally, all data were normalized by the 5 min sample.

The complete analysis of tyrosine phosphorylation was performed as described above three separate times, starting with lysates from separate 10-cm plates.

## **Results**

### **Overview of insulin-elicited tyrosine phosphorylation**

To quantify temporal dynamics of tyrosine phosphorylation in the insulin signaling network, we have immunoprecipitated stable isotope coded, tyrosine phosphorylated peptides from 3T3-L1 adipocytes stimulated with insulin for either 0, 5, 15 or 45 minutes (Figure 1). IMAC-LC-MS/MS analysis of the immunoprecipitated samples generated quantitative, temporal phosphorylation profiles for 126 peptides from 89 proteins. More than 80% of the peptides were quantified from at least two of the three biological

replicates with an average standard deviation of 10% for the three analyses (see supplementary material, Table 2).

All the sites identified and quantified in this study are listed in Table 1 according to their changes in phosphorylation after 5 min insulin stimulation relative to control (no insulin stimulation). Table 2 of the supplementary material provides a complete presentation of the data. In the description of the results given below, if the supporting data is not presented in a table or figure it can be found in Table 1 of the text and/or Table 2 of the supplementary material.

An overview of the results is as follows. Of the 122 sites in 89 proteins that were analyzed, the phosphorylation level of 86 sites in 68 proteins increased by a factor of 1.3 or more in response to insulin, while 3 sites on 3 proteins decreased by a factor of 1.3 or more. The remaining 33 sites showed less than 1.3-fold change in phosphorylation after 5 min insulin treatment. Among the 89 sites that were altered in their extent of phosphorylation more than 1.3-fold in response to insulin, 38 sites have not previously been identified as sites of tyrosine phosphorylation in any context. Moreover, among the 51 responsive sites previously identified in any context, there were 20 sites previously known to undergo a change in tyrosine phosphorylation in response to insulin or the closely related insulin-like growth factor I (IGF-I). The remaining 31 sites of tyrosine phosphorylation have been identified in other contexts but were not previously known to be affected by insulin treatment. Thus, overall we have identified 69 sites with a response of at least 1.3-fold that are either entirely novel or novel in the context of insulin action.

Especially notable in the dataset are 12 peptides that increased in phosphorylation by greater than 10-fold following 5 minutes of insulin stimulation (Table 2). These included all the peptides containing sites identified on the insulin receptor itself. In addition, several sites on proteins related to the MAPK pathway were found in this group: Y1171 on IRS-1 and Y660 on GRB2-associated binding protein (Gab) 1, two sites with very similar sequences (pYI/LDLDL) that bind the tyrosine phosphatase SHP-2 and thereby participate in activation of the MAPK pathway (9; 10), Y53 on Sprouty4, a site known to have inhibitory effect on MAPK activation (11); and the doubly phosphorylated (T202 and Y204, T185 and Y187), active forms of extracellular signal-regulated kinase (ERK) 1 and 2 (12). Three other phosphorylation sites were also found to have greater than 10-fold increase in phosphorylation: Y618 on APS, an adaptor protein linking the insulin receptor to Cbl binding (13); Y521 on Munc18c, a novel site on this protein which is involved in the fusion of GLUT4 vesicles with the plasma membrane (14); and Y1640 on Cdc42bpb, a novel site on this serine kinase, which may act as a downstream effector of Cdc42 in cytoskeleton reorganization (15). In the following sections we describe in more detail various sets of tyrosine phosphorylation sites.

### **The head of the pathway: insulin receptor and substrates of the insulin receptor**

Following ligand binding, the insulin receptor autophosphorylates on selected tyrosine residues, increasing kinase activity and recruiting adaptor proteins and substrates. We detected the singly and doubly phosphorylated forms of the catalytic loop of the kinase domain (including Y1175, 1179, 1180) with strong increase in phosphorylation up to 5 min and slight decrease to 45 min. In vitro, the triply phosphorylated form has been

reported to lead to full activation of the phosphotransferase activity; however, in vivo, the doubly phosphorylated form was found to be the major form (16). The C-terminal tyrosines 1345 and 1351 were also identified to be phosphorylated with a time-profile comparable to the sites in the catalytic loop. Those two sites have been reported to be involved in the regulation of the phosphotransferase activity of the insulin receptor (17).

IRS-1, IRS-2, Src homology 2 domain containing transforming protein C (SHC), Gab1, and APS are insulin receptor substrate/scaffolding proteins, the tyrosine phosphorylation of which connects the activation of the insulin receptor to specific pathways (1; 2; 10; 18; 19). Mouse knockouts of IRS-1 and IRS-2 have marked phenotypes that show these two IRS's play particularly prominent roles in insulin signaling (20). As expected, insulin caused a marked increase in the phosphorylation of one or more tyrosines on each of these substrate/scaffolding proteins. In the case of IRS-1, we were able to monitor the phosphorylation of 4 (Y460, Y935, Y983, Y1171) of the 10 tyrosine phosphorylation sites previously reported for mouse, rat, or human IRS-1 (PhosphoSite). Three of the sites were in the pYXXM motif, which is known to bind to the SH2 domains of the regulatory subunit of PI3K, and, as noted above, the fourth (Y1171) is a binding site for SHP-2 (10). They all showed maximal phosphorylation after 5 min insulin stimulation followed by a slight decrease with longer insulin stimulation. The peptide containing phosphorylation of Y460 demonstrated a greater decrease (to about 50% of maximum level), which was most likely due to the appearance of the doubly phosphorylated form (T448/Y460) with maximum intensity after 15 min stimulation. The T448 site has not previously been reported and its function is not known. However, as noted in the Introduction, there are many phosphorylation sites on

serine residues of IRS-1 which have been shown to alter its extent of tyrosine phosphorylation (3; 4).

In the case of IRS-2, we identified and quantified 6 tyrosine phosphorylation sites: Y594, Y628, Y649, Y671, Y734, Y758, and Y814. Remarkably, although the sites of tyrosine phosphorylation on IRS-2 have been inferred by comparison to those on IRS-1 (21), to our knowledge they have not been previously determined. All but one of these sites is in the motif pYXXM, which binds to SH2 domains of the regulatory subunit of PI3K. For all of them with exception of Y671, phosphorylation increased more than 2-fold from 0 min to 5 min followed by mostly constant levels up to 45 min. Y671 showed only slight increase from 0 to 5 min and Y734 decreased slightly from 5 to 45 minutes. However, the peptide containing Y734 was also observed in the doubly phosphorylated form with a serine phosphorylation at position 727 or 728; the doubly phosphorylated peptide slightly increased (20%) from 5 to 45 min, potentially offsetting the decrease of the singly phosphorylated form. As described above, two other substrate/scaffolding proteins, Gab1 and APS showed a marked increase in tyrosine phosphorylation. In addition, there was an 8-fold increase in the tyrosine phosphorylation of SHC, which generates a motif that binds to the adaptor protein Grb2 and contributes to activation of the MAPK pathway (22).

### **Proteins associated with the insulin receptor and/or the IRS's**

In addition to the substrates of the insulin receptor described above, insulin treatment caused increases in tyrosine phosphorylation on a number of other proteins known to be associated with the insulin receptor and/or its scaffolding substrates and to participate in

insulin signaling. The tyrosine phosphatases, SHP-1, which can associate directly with the insulin receptor, and SHP-2, which associates with the IRS's and Gab1, underwent tyrosine phosphorylation on previously identified sites (23; 24). The adaptor protein, Crk and, to a small extent, the related adaptor protein CrkL, were tyrosine phosphorylated on previously undescribed sites. Crk and CrkL are known to associate with both the insulin receptor and the IRS's (25; 26). The alpha-type 85 kDa regulatory subunit of PI3K exhibited approximately 1.5 fold increase in tyrosine phosphorylation of Y467 and Y580. Y580, but not Y467 (note that this peptide could be derived from either p85- $\alpha$  or p55- $\gamma$ ), has previously been reported to be phosphorylated by the insulin receptor (27). PI3K binds through the SH2 domains on its regulatory subunit to the IRS's and is thereby activated to produce the key signaling lipid, PtdIns 3,4,5-trisphosphate, which in turn activates the kinase Akt (1; 2). SHIP2, a phosphatase for the 5 phosphoryl group on the signaling lipid PtdIns 3,4,5 trisphosphate, showed an 8-fold increase in phosphorylation on Tyr 887, another site not previously identified as responsive to insulin. SHIP2 binds to SHC, and may participate in shutting down insulin signaling through the PI3K/Akt pathway (28). Nck 1 and 2, closely related adaptor proteins that bind to IRS-1 and may serve as a link to the cytoskeleton (29; 30), increased in tyrosine phosphorylation on a single site approximately 1.8 fold. This site on Nck has previously been identified to undergo phosphorylation in response to EGF, but not insulin (5). Fer, a cytoplasmic tyrosine kinase that associates with IRS-1 in insulin-treated adipocytes (31), exhibited a 1.7 fold increase in phosphorylation on Y402. Finally, in contrast to the other proteins in this section, the Src family tyrosine kinase Fyn, which associates with tyrosine phosphorylated IRS-1 (32), underwent a 40% decrease in phosphorylation on Y417 over the 45 min of insulin exposure. This site is

due to autophosphorylation and increases kinase activity (33), so dephosphorylation may be associated with reduced Fyn kinase activity<sup>a</sup>.

(<sup>a</sup> The peptide containing this site is also found in three other Src tyrosine kinase family members, Yes, Src and Lck. We have assigned this site to Fyn based on previous reports linking Fyn to IRS-1, but it is possible that the quantification of this site may reflect the sum total of these Src family members.)

### **Other known insulin-elicited phosphotyrosine proteins in adipocytes**

Among the pTyr proteins, there is a group that have previously been identified as undergoing insulin-stimulated tyrosine phosphorylation in adipocytes, but whose roles in signaling, if any, are less clear. This group consists of caveolin 1 and 2 (34; 35), PTRF (36), Syncrip (37), and fatty acid binding protein 4 (also known as aP2) (38). Caveolin 1 and 2 and PTRF are major protein components of the caveolar regions in the plasma membrane, which also contain insulin receptors (34; 39). In this regard, we also found a novel insulin-elicited phosphorylation on another caveolar protein, known as sdr. Sdr has previously been found to be the protein in caveolae that binds protein kinase C (40). The sites of insulin-stimulated phosphorylation on caveolin 1/2 and fatty acid binding protein 4, but not those on PTRF and Syncrip, have been previously identified.

### **Proteins not previously associated with the insulin signaling network**

In addition to the many proteins and phosphorylation sites which have been associated with insulin signaling, a substantial portion of the phosphorylation sites are on proteins that have not previously been reported to be directly involved in insulin signaling. In this section, we describe some, but not all, of these.

A major effect of insulin in adipocytes is the stimulation of glucose transport. The basis for this effect is the rapid introduction of additional glucose transporters of the GLUT4 type into the plasma membrane in response to insulin. The latter is achieved via the insulin-triggered movement of specialized intracellular vesicles containing GLUT4 to the plasma membrane and their fusion therewith (41). This process is referred to as GLUT4 translocation. Thus, it is of considerable interest that we found four proteins previously implicated in GLUT 4 translocation, Syntaxin4, Munc18c, EH domain-containing protein 2 (EHD2), and Annexin II, to be tyrosine phosphorylated in response to insulin (Table 1, Figure 2). Syntaxin4 is the plasma membrane snare protein that associates with the snare VAMP2 on GLUT4 vesicles (41). Munc18c associates with syntaxin4 and thereby may inhibit the binding of GLUT4 vesicles to syntaxin4 in the absence of insulin (14). EHD2 has been found to associate with GLUT4 (42), and it participates in GLUT4 endocytosis (43). Annexin II appears to be involved in GLUT4 translocation in a way that is not yet defined (44). Current evidence indicates that the signaling pathway to GLUT4 translocation proceeds from the insulin receptor through PI3K and the serine kinase Akt, which is not known to stimulate any tyrosine kinase (45). Thus, it is unclear whether any of these tyrosine phosphorylation sites are part of the signaling network leading to GLUT4 translocation, but because they are on proteins of the trafficking machinery, they deserve consideration.

Two transporters, a K-Cl cotransporter (Slc12a4) and an amino acid transporter (Slc38a2, SAT2), were tyrosine phosphorylated in response to insulin. Insulin has been reported to stimulate both of these transport systems. However, in the case of the K-Cl transporter, the basis for the stimulation appears to be an increase in transporter mRNA

(46); and in the case of the amino acid transporter, translocation from an internal source, similar to that for GLUT4, has been found to underlie the stimulation (47). It may be that tyrosine phosphorylation also contributes to the stimulation.

A group of four of the stimulated pTyr proteins may participate in adhesions between adipocytes. These are three membrane-associated guanylate kinases (MPP1, MPP7, and SAP102), members of a family of proteins known to be involved in cell-cell adhesion (48), and the adipocyte adhesion protein (ASP5), a transmembrane protein that has been shown to participate in cell aggregation (49). Thus, it is possible that insulin treatment may alter the adipocyte/adipocyte interactions.

### **Temporal dynamics of phosphorylation in response to insulin stimulation**

Figure 3 summarizes the insulin signaling network with the pTyr sites detected in this study coded to show the temporal dynamics of the phosphorylation sites. Among the pTyr sites that showed an initial increase of at least 1.3-fold, most sites exhibited stable phosphorylation levels from 5 to 45 minutes. However, a group of sites reached maximum phosphorylation at 5 min followed by a decrease of 40% or more over the remainder of the time course, while another group increased in phosphorylation throughout the time course, reaching at least 40% higher values after 45 min compared to 5 min insulin stimulation (Figure 4). Among the sites that decrease in phosphorylation are a set of sites involved in the activation of ERK1/2: the activating pTEpY site on the ERK1/2 themselves; Y628 and Y660 on Gab1, to which SHP-2, a protein that is involved in ERK activation, binds (9); and Y53 on Sprouty4, a phosphorylation required for Sprouty inhibition of the MAP kinase pathway (11). The decrease in the phosphorylation

of the ERK1/2 with time in 3T3-L1 adipocytes has been shown previously by immunoblotting with a phosphopeptide-specific antibody (50) and has been attributed to feedback phosphorylation of upstream kinases and the Ras guanine nucleotide exchange protein Sos that inhibit the MAPK pathway (51).

Sites that increase in phosphorylation throughout the time course (Figure 4b) also cluster into proteins with similarities. There are two likely RNA binding proteins, Syncrip and Hdlbp; and there are three membrane-associated guanylate kinases, Mpp 1 and 7, and SAP102. In addition, annexin II, which is in this group, is similar to the membrane-associated guanylate kinases in that all are peripheral membrane proteins associated with the plasma membrane (48; 52).

It is interesting that sites with similar temporal profiles appear to group together in modules within the signaling network. We have made the same observation in the EGF receptor signaling network (5). Such temporal analysis has the potential to reveal functions for previously uncharacterized sites and proteins.

## **Discussion**

This study is, to date, the most comprehensive analysis of the effect of insulin stimulation on site-specific protein tyrosine phosphorylation. We chose to use 3T3-L1 adipocytes for the analysis, since this cell type has been extensively studied, is highly insulin-responsive, and is a model for the animal fat cell. Cells were continuously exposed to insulin for 0, 5, 15 or 45 minutes. Phosphotyrosine peptide immunoprecipitation combined with iTRAQ stable isotope labeling and IMAC-LC-MS/MS

produced quantitative temporal phosphorylation profiles for a large proportion of the sites and proteins in the insulin signaling network. For instance, we detected phosphorylation on many of the previously known sites of insulin-elicited tyrosine phosphorylation on known proteins. Identification of these sites provides validation of the method. It is worth noting that not every previously known site was detected in this analysis, due to a variety of reasons, including incompatibility with IMAC-LC/MS/MS analysis or low signal level for a given peptide. In several cases (eg. c-Cbl Y369, Gab-1 Y407), sites were identified but could not be quantified due to low signal level for iTRAQ marker ions or interfering, co-eluting peptides. In addition to previously known sites, we found 66 sites with at least 1.3-fold increase in phosphorylation upon 5 min insulin stimulation that had not previously been known to be insulin-responsive. Thus, insulin-elicited tyrosine phosphorylation is much more extensive than previously known.

The significance for insulin action of tyrosine phosphorylation on each of the newly discovered sites remains to be determined. The present study offers many encouraging leads, such as the tyrosine phosphorylation of a group of proteins that are components in the trafficking machinery for GLUT4. The elucidation of the function of each tyrosine phosphorylation will require an in-depth investigation of the particular site on the particular protein. A general approach to this problem is to knockdown the protein in question, replace it with mutant protein containing non-phosphorylatable phenylalanine in place of tyrosine, and examine the effect of the replacement on insulin action. Clearly, further characterization of these novel sites and proteins will result in a significant expansion of our knowledge of the insulin signaling network.

In the future, application of this approach to the investigation of insulin signaling in various tissues of normal and diabetic mice, such as adipose tissue, muscle, and liver, will be a powerful approach to identify tissue-specific sites of tyrosine phosphorylation and the specific alterations in tyrosine phosphorylation in the diabetic state.

### **Acknowledgments**

We thank other members of the White lab and Sampsa Hautaniemi in the Lauffenburger lab at MIT for their assistance and helpful discussions. This work was supported by National Institutes of Health Grant DK42816.

## References

1. Pirola L, Johnston AM, Van Obberghen E: Modulation of insulin action. *Diabetologia* 47:170-184, 2004
2. Saltiel AR, Kahn CR: Insulin signalling and the regulation of glucose and lipid metabolism. *Nature* 414:799-806, 2001
3. Gual P, Le Marchand-Brustel Y, Tanti JF: Positive and negative regulation of insulin signaling through IRS-1 phosphorylation. *Biochimie* 87:99-109, 2005
4. Zick Y: Uncoupling insulin signalling by serine/threonine phosphorylation: a molecular basis for insulin resistance. *Biochem Soc Trans* 32:812-816, 2004
5. Zhang Y, Wolf-Yadlin A, Ross PL, Pappin DJ, Rush J, Lauffenburger DA, White FM: Time-resolved mass spectrometry of tyrosine phosphorylation sites in the epidermal growth factor receptor signaling network reveals dynamic modules. *Mol Cell Proteomics* 4:1240-1250, 2005
6. Frost SC, Lane MD: Evidence for the involvement of vicinal sulfhydryl groups in insulin-activated hexose transport by 3T3-L1 adipocytes. *J Biol Chem* 260:2646-2652, 1985
7. Gordon JA: Use of vanadate as protein-phosphotyrosine phosphatase inhibitor. *Methods Enzymol* 201:477-482, 1991
8. Martin SE, Shabanowitz J, Hunt DF, Marto JA: Subfemtomole MS and MS/MS peptide sequence analysis using nano-HPLC micro-ESI fourier transform ion cyclotron resonance mass spectrometry. *Anal Chem* 72:4266-4274, 2000
9. Cunnick JM, Mei L, Doupnik CA, Wu J: Phosphotyrosines 627 and 659 of Gab1 constitute a bisphosphoryl tyrosine-based activation motif (BTAM) conferring binding and activation of SHP2. *J Biol Chem* 276:24380-24387, 2001
10. White MF: IRS proteins and the common path to diabetes. *Am J Physiol Endocrinol Metab* 283:E413-422, 2002
11. Kim HJ, Bar-Sagi D: Modulation of signalling by Sprouty: a developing story. *Nat Rev Mol Cell Biol* 5:441-450, 2004
12. Her JH, Lakhani S, Zu K, Vila J, Dent P, Sturgill TW, Weber MJ: Dual phosphorylation and autophosphorylation in mitogen-activated protein (MAP) kinase activation. *Biochem J* 296 ( Pt 1):25-31, 1993
13. Ahn MY, Katsanakis KD, Bheda F, Pillay TS: Primary and essential role of the adaptor protein APS for recruitment of both c-Cbl and its associated protein CAP in insulin signaling. *J Biol Chem* 279:21526-21532, 2004
14. Kanda H, Tamori Y, Shinoda H, Yoshikawa M, Sakaue M, Udagawa J, Otani H, Tashiro F, Miyazaki J, Kasuga M: Adipocytes from Munc18c-null mice show increased sensitivity to insulin-stimulated GLUT4 externalization. *J Clin Invest* 115:291-301, 2005
15. Leung T, Chen XQ, Tan I, Manser E, Lim L: Myotonic dystrophy kinase-related Cdc42-binding kinase acts as a Cdc42 effector in promoting cytoskeletal reorganization. *Mol Cell Biol* 18:130-140, 1998
16. White MF, Shoelson SE, Keutmann H, Kahn CR: A cascade of tyrosine autophosphorylation in the beta-subunit activates the phosphotransferase of the insulin receptor. *J Biol Chem* 263:2969-2980, 1988
17. Tennagels N, Bergschneider E, Al-Hasani H, Klein HW: Autophosphorylation of the two C-terminal tyrosine residues Tyr1316 and Tyr1322 modulates the activity of the insulin receptor kinase in vitro. *FEBS Lett* 479:67-71, 2000
18. Holgado-Madruga M, Emler DR, Moscatello DK, Godwin AK, Wong AJ: A Grb2-associated docking protein in EGF- and insulin-receptor signalling. *Nature* 379:560-564, 1996
19. Ahmed Z, Pillay TS: Functional effects of APS and SH2-B on insulin receptor signalling. *Biochem Soc Trans* 29:529-534, 2001
20. Biddinger SB, Kahn CR: From Mice to Men: Insights into the Insulin Resistance Syndromes. *Annu Rev Physiol*, 2005
21. Sun XJ, Wang LM, Zhang Y, Yenush L, Myers MG, Jr., Glasheen E, Lane WS, Pierce JH, White MF: Role of IRS-2 in insulin and cytokine signalling. *Nature* 377:173-177, 1995
22. Sasaoka T, Kobayashi M: The functional significance of Shc in insulin signaling as a substrate of the insulin receptor. *Endocr J* 47:373-381, 2000
23. Uchida T, Matozaki T, Noguchi T, Yamao T, Horita K, Suzuki T, Fujioka Y, Sakamoto C, Kasuga M: Insulin stimulates the phosphorylation of Tyr538 and the catalytic activity of PTP1C, a protein tyrosine phosphatase with Src homology-2 domains. *J Biol Chem* 269:12220-12228, 1994
24. Stein-Gerlach M, Kharitonov A, Vogel W, Ali S, Ullrich A: Protein-tyrosine phosphatase 1D modulates its own state of tyrosine phosphorylation. *J Biol Chem* 270:24635-24637, 1995
25. Feller SM: Crk family adaptors-signalling complex formation and biological roles. *Oncogene* 20:6348-6371, 2001

26. Klammt J, Barnikol-Oettler A, Kiess W: Mutational analysis of the interaction between insulin receptor and IGF-I receptor with c-Crk and Crk-L in a yeast two-hybrid system. *Biochem Biophys Res Commun* 325:183-190, 2004
27. Hayashi H, Nishioka Y, Kamohara S, Kanai F, Ishii K, Fukui Y, Shibasaki F, Takenawa T, Kido H, Katsunuma N, et al.: The alpha-type 85-kDa subunit of phosphatidylinositol 3-kinase is phosphorylated at tyrosines 368, 580, and 607 by the insulin receptor. *J Biol Chem* 268:7107-7117, 1993
28. Dyson JM, Kong AM, Wiradjaja F, Astle MV, Gurung R, Mitchell CA: The SH2 domain containing inositol polyphosphate 5-phosphatase-2: SHIP2. *Int J Biochem Cell Biol* 37:2260-2265, 2005
29. Tu Y, Liang L, Frank SJ, Wu C: Src homology 3 domain-dependent interaction of Nck-2 with insulin receptor substrate-1. *Biochem J* 354:315-322, 2001
30. Rivera GM, Briceno CA, Takeshima F, Snapper SB, Mayer BJ: Inducible clustering of membrane-targeted SH3 domains of the adaptor protein Nck triggers localized actin polymerization. *Curr Biol* 14:11-22, 2004
31. Iwanishi M, Czech MP, Cherniack AD: The protein-tyrosine kinase fer associates with signaling complexes containing insulin receptor substrate-1 and phosphatidylinositol 3-kinase. *J Biol Chem* 275:38995-39000, 2000
32. Sun XJ, Pons S, Asano T, Myers MG, Jr., Glasheen E, White MF: The Fyn tyrosine kinase binds Irs-1 and forms a distinct signaling complex during insulin stimulation. *J Biol Chem* 271:10583-10587, 1996
33. Roskoski R, Jr.: Src protein-tyrosine kinase structure and regulation. *Biochem Biophys Res Commun* 324:1155-1164, 2004
34. Kimura A, Mora S, Shigematsu S, Pessin JE, Saltiel AR: The insulin receptor catalyzes the tyrosine phosphorylation of caveolin-1. *J Biol Chem* 277:30153-30158, 2002
35. Lee H, Park DS, Wang XB, Scherer PE, Schwartz PE, Lisanti MP: Src-induced phosphorylation of caveolin-2 on tyrosine 19. Phospho-caveolin-2 (Tyr(P)19) is localized near focal adhesions, remains associated with lipid rafts/caveolae, but no longer forms a high molecular mass hetero-oligomer with caveolin-1. *J Biol Chem* 277:34556-34567, 2002
36. Ibarrola N, Molina H, Iwahori A, Pandey A: A novel proteomic approach for specific identification of tyrosine kinase substrates using [<sup>13</sup>C]tyrosine. *J Biol Chem* 279:15805-15813, 2004
37. Hresko RC, Mueckler M: Identification of pp68 as the Tyrosine-phosphorylated Form of SYNCRIP/NSAP1. A cytoplasmic RNA-binding protein. *J Biol Chem* 277:25233-25238, 2002
38. Hresko RC, Hoffman RD, Flores-Riveros JR, Lane MD: Insulin receptor tyrosine kinase-catalyzed phosphorylation of 422(ap2) protein. Substrate activation by long-chain fatty acid. *J Biol Chem* 265:21075-21085, 1990
39. Aboulaich N, Vainonen JP, Stralfors P, Vener AV: Vectorial proteomics reveal targeting, phosphorylation and specific fragmentation of polymerase I and transcript release factor (PTRF) at the surface of caveolae in human adipocytes. *Biochem J* 383:237-248, 2004
40. Mineo C, Ying YS, Chapline C, Jaken S, Anderson RG: Targeting of protein kinase Calpha to caveolae. *J Cell Biol* 141:601-610, 1998
41. Watson RT, Kanzaki M, Pessin JE: Regulated membrane trafficking of the insulin-responsive glucose transporter 4 in adipocytes. *Endocr Rev* 25:177-204, 2004
42. Park SY, Ha BG, Choi GH, Ryu J, Kim B, Jung CY, Lee W: EHD2 interacts with the insulin-responsive glucose transporter (GLUT4) in rat adipocytes and may participate in insulin-induced GLUT4 recruitment. *Biochemistry* 43:7552-7562, 2004
43. Guilherme A, Soriano NA, Furcinitti PS, Czech MP: Role of EHD1 and EHBP1 in perinuclear sorting and insulin-regulated GLUT4 recycling in 3T3-L1 adipocytes. *J Biol Chem* 279:40062-40075, 2004
44. Huang J, Hsia SH, Imamura T, Usui I, Olefsky JM: Annexin II is a thiazolidinedione-responsive gene involved in insulin-induced glucose transporter isoform 4 translocation in 3T3-L1 adipocytes. *Endocrinology* 145:1579-1586, 2004
45. Welsh GI, Hers I, Berwick DC, Dell G, Wherlock M, Birkin R, Leney S, Tavaré JM: Role of protein kinase B in insulin-regulated glucose uptake. *Biochem Soc Trans* 33:346-349, 2005
46. Shen MR, Lin AC, Hsu YM, Chang TJ, Tang MJ, Alper SL, Ellory JC, Chou CY: Insulin-like growth factor 1 stimulates KCl cotransport, which is necessary for invasion and proliferation of cervical cancer and ovarian cancer cells. *J Biol Chem* 279:40017-40025, 2004
47. Hyde R, Peyrollier K, Hundal HS: Insulin promotes the cell surface recruitment of the SAT2/ATA2 system A amino acid transporter from an endosomal compartment in skeletal muscle cells. *J Biol Chem* 277:13628-13634, 2002
48. Funke L, Dakoji S, Bredt DS: Membrane-associated guanylate kinases regulate adhesion and plasticity at cell junctions. *Annu Rev Biochem* 74:219-245, 2005

49. Eguchi J, Wada J, Hida K, Zhang H, Matsuoka T, Baba M, Hashimoto I, Shikata K, Ogawa N, Makino H: Identification of adipocyte adhesion molecule (ACAM), a novel CTX gene family, implicated in adipocyte maturation and development of obesity. *Biochem J* 387:343-353, 2005
50. Kayali AG, Austin DA, Webster NJ: Stimulation of MAPK cascades by insulin and osmotic shock: lack of an involvement of p38 mitogen-activated protein kinase in glucose transport in 3T3-L1 adipocytes. *Diabetes* 49:1783-1793, 2000
51. Waters SB, Yamauchi K, Pessin JE: Insulin-stimulated disassociation of the SOS-Grb2 complex. *Mol Cell Biol* 15:2791-2799, 1995
52. Gerke V, Moss SE: Annexins and membrane dynamics. *Biochim Biophys Acta* 1357:129-154, 1997

## Tables

**Table 1.** pTyr sites of proteins identified and quantified in this study, grouped according to their response to 5 min treatment with insulin. Sites in *italic* have not been reported previously, according to the PhosphoSite database ([www.phosphosite.org](http://www.phosphosite.org)). The gene names and the phosphorylation sites are listed. Detailed information (protein name, gi-number, quantitative data) is in supplementary material, Table 2.

<b>≥ 10x increase</b>		* SHC (+ LOC433158)	Y313	PVR	Y391
APS	Y618	SHIP-2	Y887	SAP102	Y705
Cdc42bpb	Y1640	SHP-1	Y536	Sgk269	Y632
ERK1	T203	Slc12a4	Y17	SHP-2	Y584
	Y205	Slc38a2	Y20	Slc38a2	Y41
ERK2	T183	syntaxin 4	Y115	tensin 2	Y460
	Y185	syntaxin 4	Y251	taln 1	Y1116
Gab1	Y660	* Syncrip	Y376	Tns	Y1225
* IR (+ IGFR)	Y1175, Y1179, Y1180 (1 p and 2 p')	(isoform 1+2) Zdhhc20	Y327	<b>≥ 1.3x decrease</b>	
		<b>≥ 1.3x increase</b>		Odin	Y472
IR	T1344/ Y1345 Y1351 (2 p's)	Abi-1	Y123	* Fyn (+ Src, Yes, Lck)	Y417
IR	Y1345 Y1351 (1 p)	Ack1	Y874	Tns	Y1144
IRS-1	Y1171	ATPCL	Y672	<b>&lt; 1.3x change</b>	
Munc18c	Y521	ADD1	Y550	Ack1	Y284
Spry4	Y53	* ANXA2 (+1)	Y24	CAS-L	Y165
		* ANXA2 (+1)	Y238	CrkL	Y132
		* Calm1 (+Calm2/3)	Y100	DBI	Y29
		CAV1	Y42	Dok1	Y361
		DDR2	Y436	* DYRK1A (+DYRK1B)	Y321
		EFNB1	Y316	* Erbin	Y1097
		* ELMO2 (4 isoforms)	Y48	(2 isoforms)	
		* ENO1 (+ ENO2, LOC433182, ENO3)	Y44	* eEF1A-2 (+eEF1A-1, LOC545418, LOC545767)	Y141
<b>≥ 3x increase</b>		ERK5	Y221	FAK	Y397
Odin	<i>S461</i> <i>/S462</i> Y472 (pS+ pY)	Fer	Y402	FAK	Y576
AFABP4	Y20	* GAPDH (+ many others)	Y315	FAS	Y1248
ASP5	Y333	Git2	Y512	Fer	Y715
CAV2	Y19	Glud1	Y512	* GSK3β (+GSK3α)	Y216
CAV1	Y6/Y14	Hdlbp	Y437	HIPK3	Y359
Crk	Y136	IRS-2	Y649	HIPK1	Y352
DDX3	Y69	IRS-2	S727/ S728	IRS-2	Y671
DDX3	Y104		Y734 (2 p's)	Jak2	Y570
EHD2	Y453	ITSN2	Y922	LOC226250	Y68
ERK1	Y205	* LR1	Y139	LOC226250	Y357
ERK2	Y185	(+ LOC433712, LOC433142)		LOC69225	Y86
Gab1	Y628	LOC226250	Y401	Met	Y1001
IRS-1	Y460	LOC268739	Y242	P130Cas	Y253
IRS-1	<i>T448</i>	LOC71900	Y51	P130Cas	Y414
IRS-1	Y460	Mpp7	Y417	PK3	Y105
IRS-1	Y935	Nck1	Y105	PRP4	Y849
IRS-1	Y983	Nck2	Y110	* PXN-β (+PXN-α)	Y118
IRS-2	Y734	p130Cas	Y391	Sgk223	Y196
IRS-2	Y814	P38-α	Y182	SHP-2	Y62
IRS-2	Y758	PAR-3	Y1076	* STAT3 (2 isoforms)	Y705
IRS-2	Y594	* PI3K p85-α (+p55)	Y467	tensin 2	Y682
IRS-2	Y628	PI3K p85-α	Y580	tensin 2	Y747
LPP	Y301	PTPRA	Y825	vinculin	Y822
Mpp1	Y331	PTRF	Y158	WASP	Y253
PTRF	Y310				
RAIG1	Y386				
Sdpr	Y388				

\* Sites from peptides resulting from more than one protein, based on NCBI mouse database.

**Table 2.** Temporal phosphorylation dynamics of sites with at least 10-fold increase after 5 min insulin stimulation.

Protein	Phosphorylation site	n <sup>a</sup>	0min: 5min <sup>b</sup>	5min: 5min	15min: 5min <sup>b</sup>	45min: 5min <sup>b</sup>
APS	Y618	3	0.07±0.01	1	0.98±0.09	0.82±0.17
Cdc42bpb	Y1640	3	0.09±0.01	1	0.94±0.06	0.80±0.09
ERK1	T202 Y204	3	0.05±0.00	1	0.59±0.08	0.37±0.03
ERK2	T185 Y187	3	0.07±0.02	1	0.66±0.03	0.42±0.03
Gab1	Y660	3	0.07±0.02	1	0.61±0.13	0.33±0.06
IR	Y1175 / Y1179 / Y1180 (1p)	3	0.08±0.01	1	1.05±0.04	0.82±0.12
	Y1175 / Y1179 / Y1180 (2p's)	3	0.03±0.01	1	0.99±0.06	0.81±0.08
	T1344/Y1345 Y1351 (2p's)	3	0.06±0.01	1	1.03±0.11	0.85±0.12
	Y1345 / Y1351 (1p)	1	0.07	1	1.07	0.94
IRS-1	Y1171	3	0.03±0.01	1	1.02±0.07	0.77±0.06
Munc18c	Y521	3	0.07±0.01	1	1.11±0.01	1.20±0.14
SPRY4	Y53	3	0.07±0.02	1	0.87±0.08	0.31±0.01

<sup>a</sup> Number of replicate analyses in which the site could be quantified.

<sup>b</sup> Average values are given, for single values see supplementary material

## Figure legends

**Figure 1. Methodology used to identify and quantify tyrosine phosphorylation sites upon insulin stimulation.** Adipocytes were stimulated with insulin for different times. After cell lysis and digestion, the resulting peptides were labeled with iTRAQ reagent and the samples were combined for further analysis, i.e., phosphotyrosine peptide immunoprecipitation, IMAC, LC-MS/MS. The identity of the peptide was determined from the MS/MS spectrum and the area of the tag masses 114, 115, 116, and 117 m/z was used to calculate the ratio of phosphorylated peptides at the different time points compared to 5 min insulin stimulation. The doubly phosphorylated peptide of ERK1 is shown as an example.

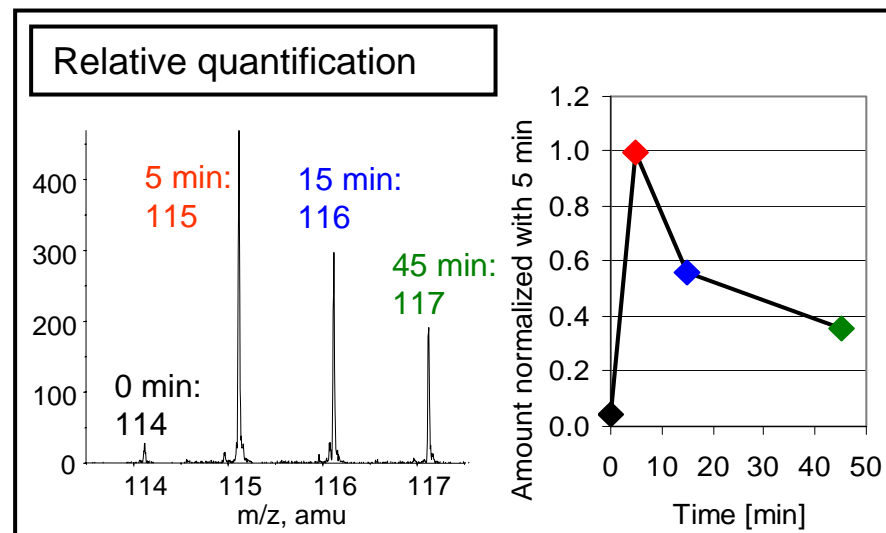
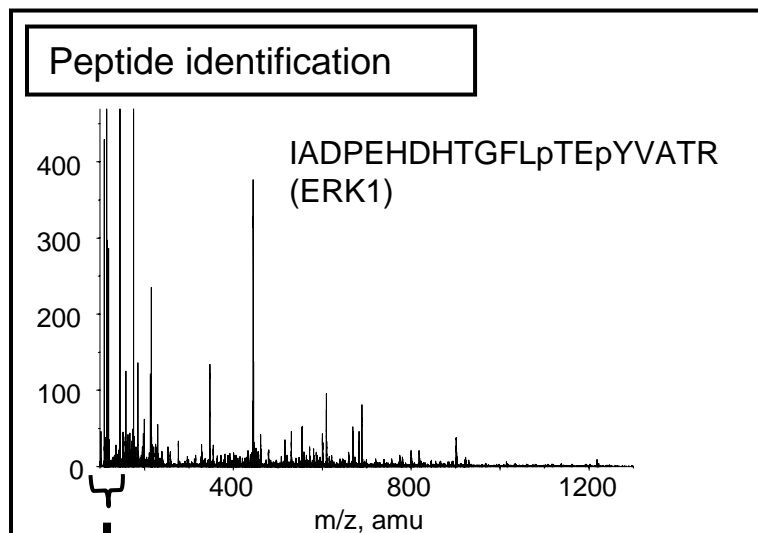
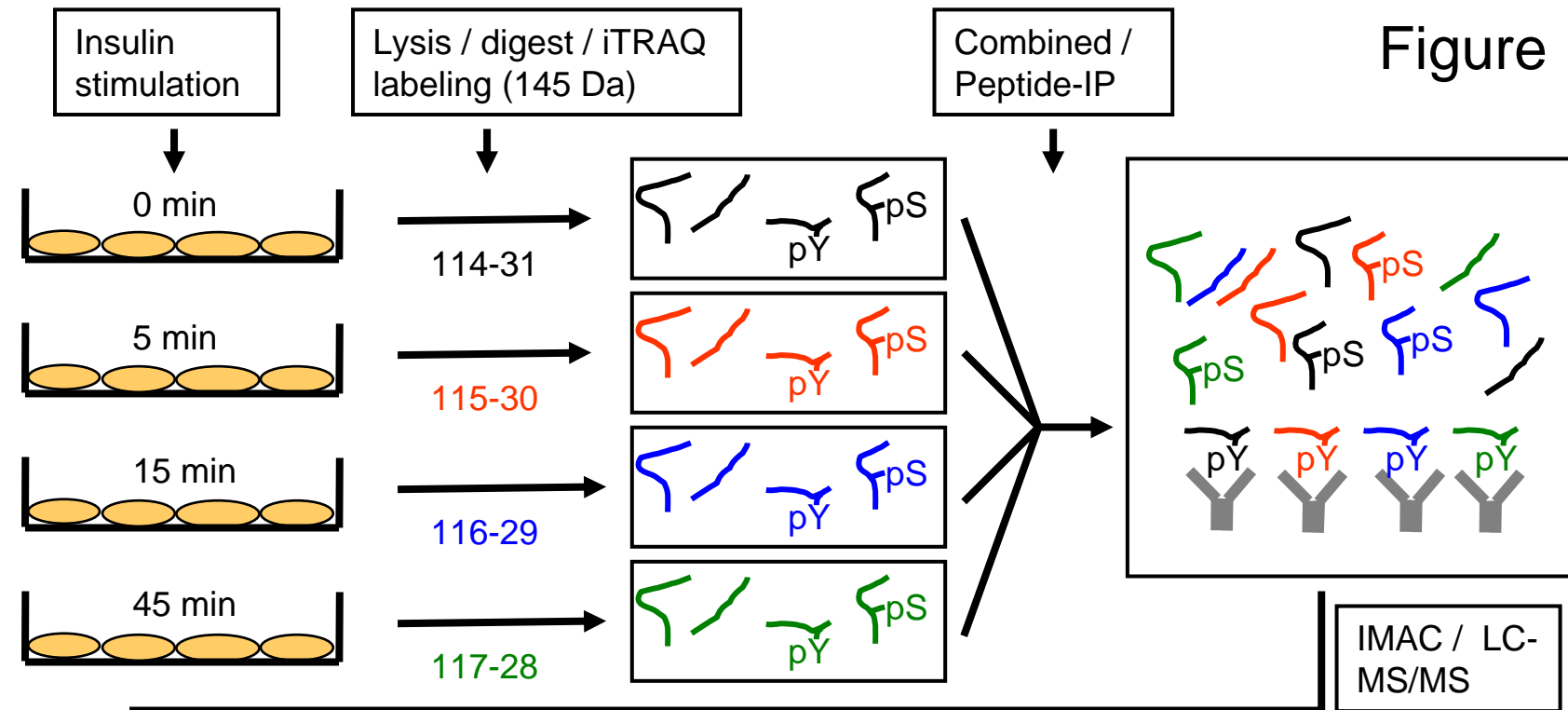
**Figure 2. MS/MS spectra and temporal profiling of tyrosine phosphorylation sites on GLUT4 translocation-related proteins.** Protein name, phosphorylation site (pY) and sequence of the peptide identified by each MS/MS spectrum are provided along with a graph indicating temporal phosphorylation profile normalized to the value at 5 min. A) m/z: +2. Data are means  $\pm$  SD from 3 experiments. B) m/z:+4. Data are from 1 experiment. C) m/z: +3. Data are means  $\pm$  SD from 3 experiments. D) m/z:+4. Data are from 1 experiment.

**Figure 3. Tyrosine phosphorylation sites identified on proteins involved in insulin signaling.** Proteins with sites identified in this study are shown in yellow. Simplified temporal dynamics of the phosphorylation sites are represented in colored small ovals connected to the proteins, with site numbers as indicated. The color in the first half shows changes between 0 and 5 min, color in the second half shows changes between

5 and 45 min, with red  $\geq 3$ -fold increase and orange  $\geq 1.3$ -fold increase, blue  $< 1.3$ -fold change and green  $\geq 1.3$ -fold decrease in phosphorylation. The insulin signaling network is adapted from (1; 2).

**Figure 4: Temporal dynamics of tyrosine phosphorylation enable grouping of co-regulated sites on proteins with similar functionality.** Phosphorylation profiles for sites showing an initial increase in phosphorylation at 5 min of more than 1.3x followed by at least 40% change to 45 min. (A) Sites that decrease after 5 min (B) Sites that increase after 5 min.

# Figure 1



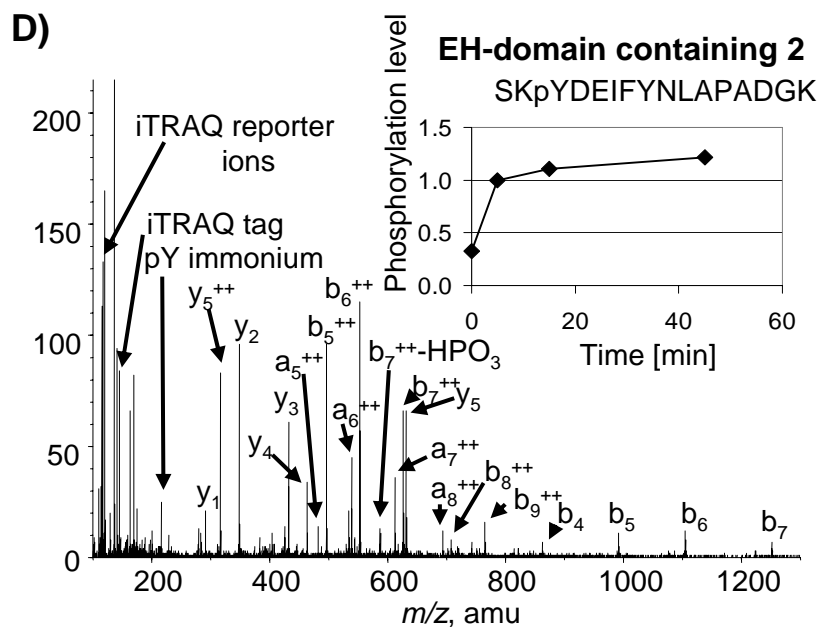
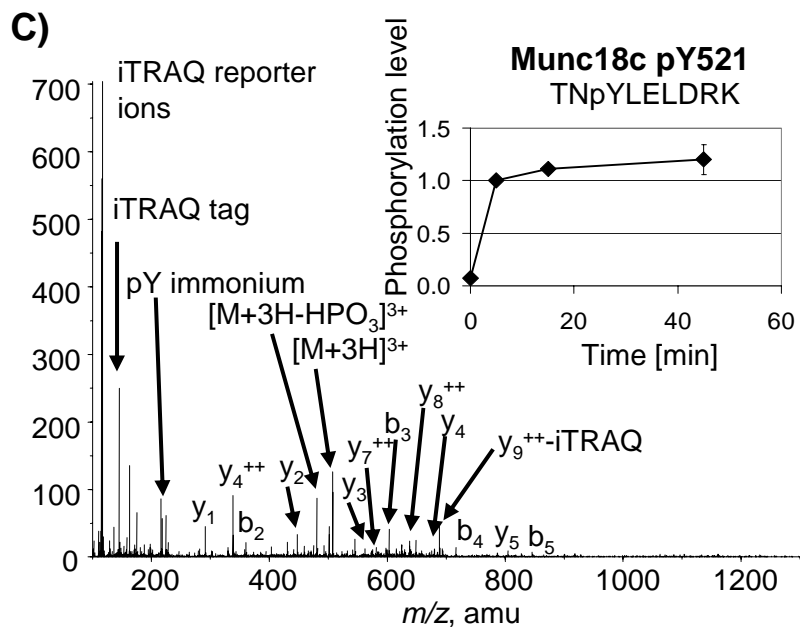
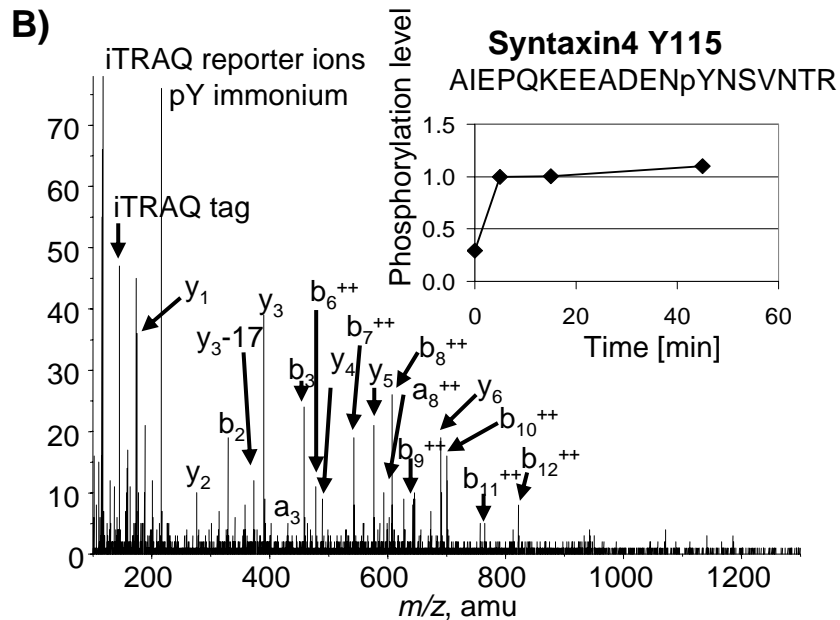
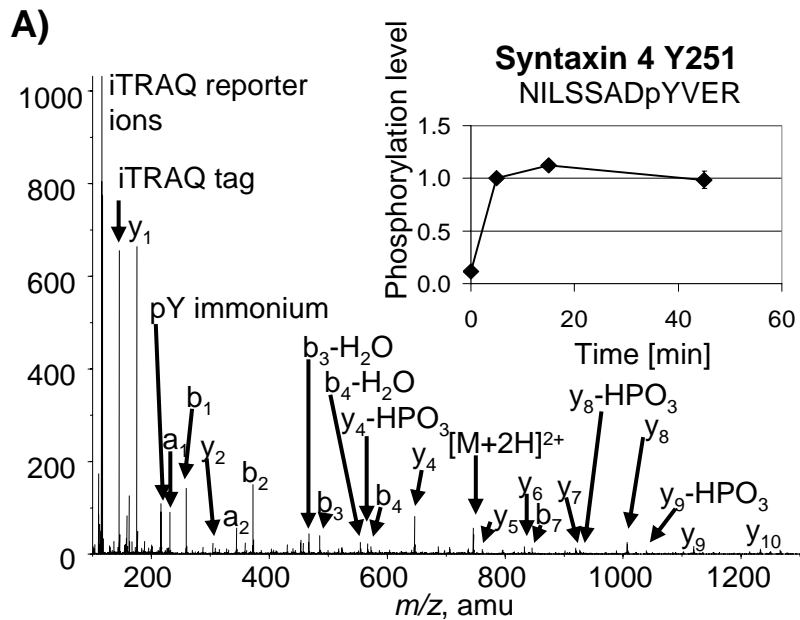


Figure 2

Figure 3

